

MVP-Shot: Multi-Velocity Progressive-Alignment Framework for Few-Shot Action Recognition

Hongyu Qu, Rui Yan, Xiangbo Shu, Haoliang Gao, Peng Huang, and Guo-Sen Xie

Abstract—Recent few-shot action recognition (FSAR) methods achieve promising performance by performing semantic matching on learned discriminative features. However, most FSAR methods focus on single-scale (*e.g.*, frame-level, segment-level, *etc.*) feature alignment, which ignores that human actions with the same semantic may appear at different velocities. To this end, we develop a novel Multi-Velocity Progressive-alignment (MVP-Shot) framework to progressively learn and align semantic-related action features at multi-velocity levels. Concretely, a Multi-Velocity Feature Alignment (MVFA) module is designed to measure the similarity between features from support and query videos with different velocity scales and then merge all similarity scores in a residual fashion. To avoid the multiple velocity features deviating from the underlying motion semantic, our proposed Progressive Semantic-Tailored Interaction (PSTI) module injects velocity-tailored text information into the video feature via feature interaction on channel and temporal domains at different velocities. The above two modules compensate for each other to predict query categories more accurately under the few-shot settings. Experimental results show our method outperforms current state-of-the-art methods on multiple standard few-shot benchmarks (*i.e.*, HMDB51, UCF101, Kinetics, and SSv2-small).

Index Terms—Few-shot action recognition, Few-shot learning, Action recognition, Pre-trained vision-language model

I. INTRODUCTION

Due to the increasing demand for video analysis in real-world scenarios, action recognition has gained significant progress [1]–[5] in recent years. Despite this, these successes still heavily rely on extensive manual data annotation and collecting these data is expensive and labor-intensive. This significant bottleneck severely constrains the broader applicability of this task. To relieve dependence on a large amount of labeled data, few-shot action recognition (FSAR) is a promising direction and has gained widespread attention [6]–[10] in recent years. It aims to recognize new categories with only a few labeled examples.

Current mainstream FSAR approaches follow the metric-based meta-learning paradigm, which maps videos into an appropriate feature space and performs feature alignment to predict action category labels. Most metric-based methods perform **frame-level alignment** [7], [9], [11]–[13] on learned discriminative frame-level features, which measure the similarity between query and support videos via diverse matching strategies [7], [11], [14]. In addition, some methods

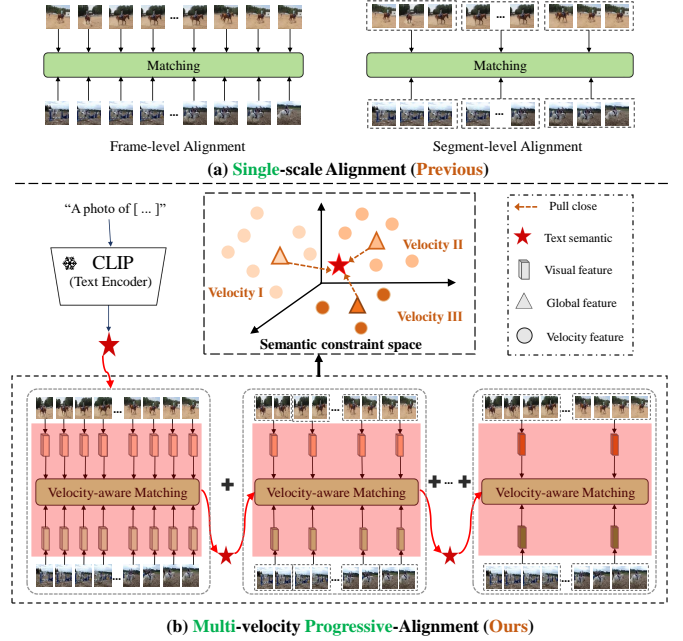


Fig. 1. The main idea of this work. (a): The previous methods focus on **single-velocity feature alignment**, such as frame-level and segment-level. (b): In our work, we capture multi-velocity feature representation and perform **multi-velocity feature alignment** to deal with action instances with diverse speeds.

perform **segment-level alignment** [15]–[17] on obtained segment-level features. Typically, TARN [15] first uniformly samples segments from videos, and performs segment-level alignment based on segment features extracted by 3D-CNN. Although existing FSAR methods have achieved remarkable performance, these methods still mainly focus on single-scale feature alignment (*i.e.*, frame-level alignment and segment-level alignment), as shown in Fig. 1(a), which is insufficient to reflect the diversity of action speeds. Therefore, these single-scale approaches often result in inaccurate matching when dealing with action instances with diverse speeds. In real-world scenarios, different individuals may perform the same action class at different velocities. Take the action “ride horse” as an example, different persons act at different velocities. Specifically from a visual perspective, certain horses may be perceived sprinting at a rapid pace, while others may be observed moving at a more leisurely walk.

In our paper, we focus on multi-velocity feature alignment in FSAR, where multi-velocity features are utilized to capture pair-wise semantic relevance at different velocity scales as shown in Fig. 1(b). With multi-velocity feature alignment, we can achieve more accurate matching to some extent in the collaboration of multiple-velocity features. However, with

H. Qu, X. Shu, H. Gao, P. Huang and G.-S. Xie are with the School of Computer Science and Engineering, Nanjing University of Science and Technology, Nanjing 210094, China. E-mail: {quhongyu, shuxb, gaohailiang, penghuang}@njust.edu.cn, gsxiehm@gmail.com. (Corresponding author: Xiangbo Shu)

R. Yan is with the Department of Computer Science and Technology, Nanjing University, Nanjing 210023, China. E-mail: ruiyan@nju.edu.cn.

only limited support videos, the learned multi-velocity action features are not up to adhere to the underlying motion semantic without extra semantic constraints. Actually, the human perception system possesses a distinctive visual mechanism known as cognitive penetrability [18]. This mechanism employs prior linguistic knowledge to adjust visual perception processing towards semantic-relevant features. Hence, we argue that it is necessary to leverage text information to avoid multi-velocity features deviating from the underlying motion semantic for the rare support samples.

Inspired by the above insights, we propose a novel **Multi-Velocity Progressive-alignment (MVP-Shot)** framework to learn and align multi-velocity action features in a progressive manner, as shown in Fig. 1(b). More specifically, we present a novel **Progressive Semantic-Tailored Interaction (PSTI)** module to capture multiple action features from different velocity scales, in which we recurrently inject velocity-tailored text information at different velocities to enhance velocity-aware semantic features. Thus rich semantic prior knowledge is fully utilized to avoid multiple velocity features deviating from the original motion semantic. To cooperate with the PSTI module, we further design a **Multi-Velocity Feature Alignment (MVFA)** module to capture pair-wise semantic similarity scores at different velocity scales, and then merge all similarity scores in a residual fashion to facilitate coherent velocity-aware matching between videos. In this way, our proposed MVP-shot combines the above two modules to compensate for each other, which enables more robust and more accurate few-shot matching.

To comprehensively evaluate our method, we conduct experiments on four gold-standard datasets (*i.e.*, HMDB51 [19], UCF101 [20], Kinetics [21], and SSv2-small [22]). We empirically prove that our approach surpasses all existing state-of-the-arts and yields solid performance gains, *e.g.*, 3.2% accuracy gains on HMDB51 dataset under the 5-way 1-shot setting. Furthermore, we perform thorough ablation studies to dissect each component, both quantitatively and qualitatively.

In summary, the main contributions of this paper are as follows:

- We propose a novel MVP-Shot framework to enhance Few-Shot Action Recognition (FSAR) matching by learning and aligning reliable multi-velocity action features in a progressive way.
- **To learn multi-velocity action features** reliably, we design a new Progressive Semantic-Tailored Interaction (PSTI) module that recurrently injects velocity-tailored text information into video features via feature interaction on different domains.
- **To align multi-velocity action features** covering different temporal dynamics, we present a new Multi-Velocity Feature Alignment (MVFA) module to measure the similarity of action features from different velocities in a residual fashion. To the best of our knowledge, this is the first work to exploit multi-velocity matching for FSAR.

The rest of this paper is organized as follows: Section §II describes the related works including few-shot image classification, few-shot action recognition, and transferring CLIP models for video recognition. Section §III presents the proposed MVP-

shot in detail for few-shot action recognition. Section §IV reports the results and analysis of extensive experiments, followed by the conclusion in Section §V.

II. RELATED WORK

In this section, we review several lines of researches closely related to the paper, including few-shot image classification (§II-A), few-shot action recognition (§II-B), and transferring CLIP models for video recognition (§II-C).

A. Few-Shot Image Classification

The few-shot learning (FSL) task, aiming to recognize new classes with limited samples, is an important research direction in computer vision. Existing FSL methods are roughly categorized into three groups: augmentation-based methods, optimization-based methods, and metric-based methods. Augmentation-based methods [23]–[25] usually learn to increase the number of training samples or features to augment model training and improve the generalization of few-shot models, mainly including hallucinating additional training examples [23] and adversarial generation [24]. Optimization-based methods [26]–[29] learn a good initialization for the model or learn to update the parameters of the model properly so that the model can quickly adapt to new tasks with limited fine-tuning updates. Typical methods include MAML [26] and other variants [27]–[29]. Metric-based methods [30]–[36] leverage visual encoders to map images into a common embedding space and compare query and support images through different distance metrics, such as Euclidean distance [30], [37] and cosine similarity [38]. For example, Prototypical Network [39] can compute the Euclidean distances between the class prototypes of the query set and support set to obtain classification results. Our work also falls into the metric-based line and tries to solve the more challenging few-shot action recognition (FSAR) with diverse spatiotemporal dependencies. Our work focuses on making full use of temporal information to obtain and align semantic-related action features at multi-velocity levels.

B. Few-Shot Action Recognition

Few-shot action recognition aims to learn to categorize an unlabeled query video into one of the action categories in the support set with limited samples. Compared to images, video has richer spatio-temporal contextual information and temporal diversity. Therefore, it is not reasonable to directly apply few-shot image classification methods to the few-shot video recognition task. The existing few-shot action recognition methods [7], [40]–[42] mainly focus on metric-based learning to exploit the temporal cues. On the one hand, some approaches [41], [43] aim to enhance feature representation for few-shot action recognition. STRM [13] utilizes the spatiotemporal enrichment module, comprising a local patch-level enrichment sub-module and a global frame-level enrichment sub-module, to learn higher-order temporal representations. ITANet [44] introduces joint spatiotemporal modeling techniques to achieve implicit temporal alignment and matching. HyRSM [7] introduces a

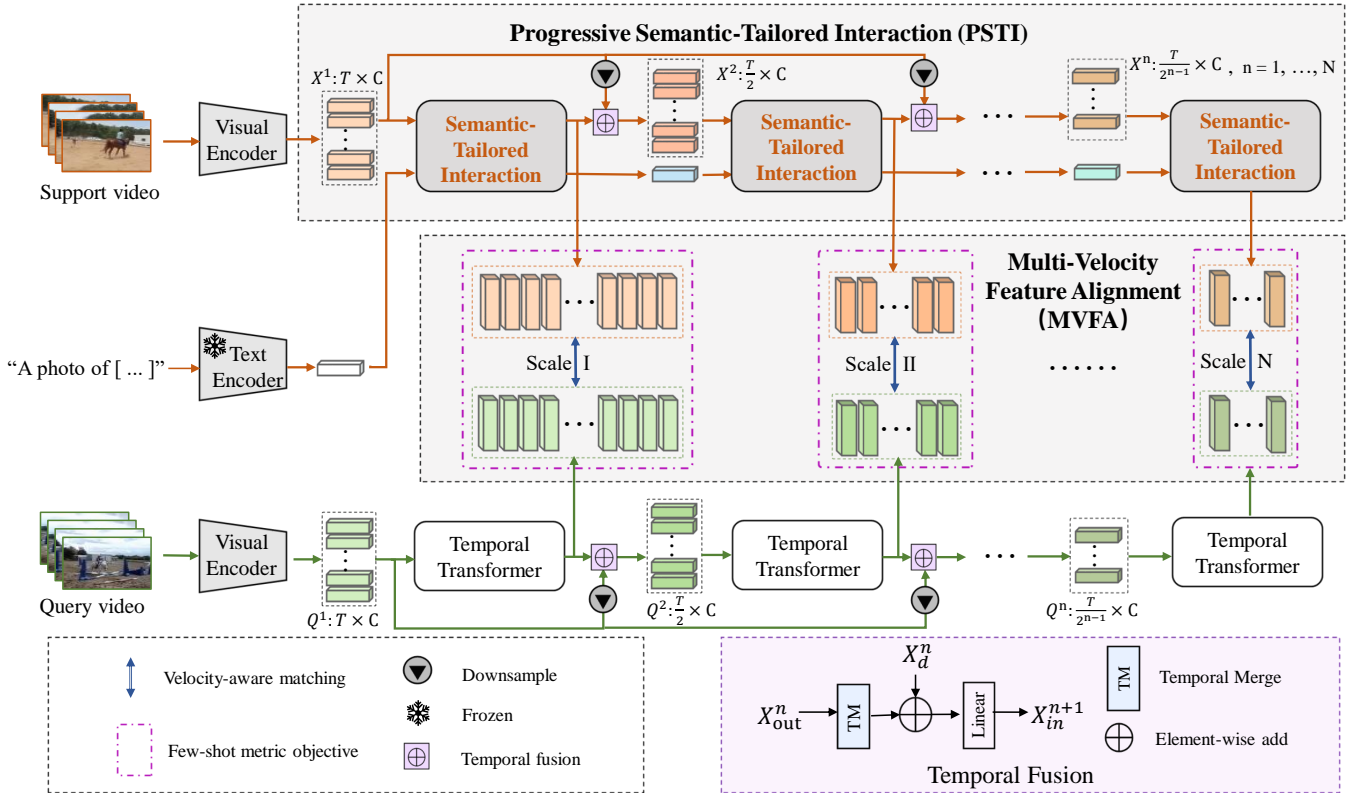


Fig. 2. The architecture of the proposed Multi-Velocity Progressive-Alignment (MVP-shot) Framework. Given the support and query videos, we first leverage a feature extractor to encode frame features. Then, based on frame features, we apply a Progressive Semantic-Tailored Interaction (PSTI) module to capture multi-velocity action features. Accordingly, we employ a Multi-Velocity Feature Alignment (MVFA) module to capture pair-wise semantic relevance at different velocity scales. For the convenience of illustration, other support videos in a few-shot task are not displayed in the figure.

novel hybrid relation module to capture task-specific features, and SloshNet [42] designs a feature fusion architecture search module to automatically search for the best combination of the low-level and high-level spatial features. On the other hand, some methods focus on class prototype matching [11], [45], [46] strategies. Among them, OTAM [11] maintains the frame order in video and aligns the two video sequences using an improved dynamic time-warping algorithm. TARN [15] achieves temporal alignment by using an attention mechanism between the segment embeddings of the videos. TRX [14] matches each query sub-sequence with all sub-sequences in the support set and thus establishes query-specific video matching. In a word, the above methods focus on frame-level alignment or segment-level alignment solely. However, these single-scale approaches do not handle action instances with diverse speeds effectively. Unlike these previous methods, our work combines multi-velocity feature representation and multi-velocity feature alignment to compensate for each other, which enables more robust and more accurate few-shot matching.

C. Transferring CLIP Models for Video Recognition

With deep learning advancements [47]–[50], significant progress has been made in the field of action recognition [51]–[54] in recent years. Recently, image-language pretraining [55], [56] has achieved remarkable progress due to its powerful visual representations aligned with rich linguistic semantics. One of the most representative works is CLIP [56], which

achieves impressive “zero-shot” transferability and generalization capacity. CLIP projects images and natural language descriptions to a common feature space through two separate encoders for contrastive learning. Thus these pre-trained models have been extended to various downstream tasks and achieve impressive performance, including image classification [32], [57] and video understanding [58], [59]. Inspired by these successes, CLIP-FSAR [60] firstly transfers CLIP for few-shot action recognition to integrate both visual features and auxiliary text features. However, CLIP models are image pre-trained models, while videos have richer spatio-temporal contextual information compared to images. Current methods only propose an additional temporal module to extend image pre-trained models, which are unable to take full advantage of temporal information in videos. To perform temporal modeling effectively, we propose a Semantic-Tailored Interaction module including two complementary mechanisms to inject semantic information into the visual features, which allow the interaction on the temporal and the channel dimensions, respectively. The Semantic-Tailored Interaction module fully utilizes semantic information of class names to obtain more discriminative video features and enhance the representation of video prototypes for few-shot learning.

III. METHOD

In this section, we first introduce the problem setup of the few-shot action recognition task (§III-A). Then, we present an

architecture overview of the proposed MVP-shot (§III-B), as shown in Fig. 2. Finally, we describe each component of our proposed method in detail (§III-C and §III-D).

A. Problem Statement

The objective of few-shot action recognition is to learn a model that generalizes its performance to identify unseen categories using only a few samples. To make the training phase more faithful to the test phase, we adopt the episodic training manner [61] for few-shot adaptation as in previous work. In each episodic task, there are two sets, which consist of support set S and query set Q . The support set consists of N different action categories, and each category comprises K support videos, which typically range from 1 to 5. The problem setting like this is termed as the N -way K -shot problem. The goal is to correctly classify the sample in the query set into one of the N categories in the support set. Specifically, in the few-shot learning setting, the whole dataset is divided into a base set $\mathcal{D}_{base} = \{(v_i, y_i), y_i \in \mathcal{C}_{base}\}$ and a novel set $\mathcal{D}_{novel} = \{(v_i, y_i), y_i \in \mathcal{C}_{novel}\}$, wherein y_i represents the action label of video v_i . Note that the categories of \mathcal{D}_{base} and \mathcal{D}_{novel} are sample-wise non-overlapping, $\mathcal{C}_{base} \cap \mathcal{C}_{novel} = \emptyset$. We utilize \mathcal{D}_{base} to train our network for obtaining a robust and generalized model, and we use \mathcal{D}_{novel} to evaluate the effectiveness of the proposed method.

B. Architecture Overview

The overall architecture of our proposed MVP-shot is illustrated in Figure 2. In a standard N -way K -shot episodic task, there is a support $S = \{s_1, s_2, \dots, s_{N \times K}\}$ consisting of N action categories and K videos per category, where $s_i \in \mathbb{R}^{T \times 3 \times H \times W}$ and T is the number of sparsely sampled video frames. For the convenience of formulation, we consider the N -way 1-shot task to present our framework, and the query set Q contains a single video q . We first adopt the visual encoder of CLIP to generate the support features $F_S = \{f_{s_1}, f_{s_2}, \dots, f_{s_N}\}$ and query feature f_q , where $f_i = \{f_i^1, f_i^2, \dots, f_i^T\}$, $f_i^j \in \mathbb{R}^C$ and C is the channel number. We also use the text encoder of CLIP to obtain the textual embeddings of corresponding category natural language descriptions. Then we propose a Progressive Semantic-Tailored Interaction (PSTI) module to obtain semantic-related action features from different velocities. With such multi-velocity feature representation, we utilize a Multi-Velocity Feature Alignment (MVFA) module to measure the similarity of the specific semantic information at different temporal scales and produce the final predicted probabilities after a fusion operation. In our proposed MVP-shot, visual features from different velocity scales are complementary, and they work collaboratively to significantly improve classification performance.

C. Progressive Semantic-Tailored Interaction

For some challenging action categories with diverse speeds, only utilizing single-velocity temporal features may lead to less satisfactory video classification results. Thus, we propose a novel Progressive Semantic-Tailored Interaction (PSTI) module to

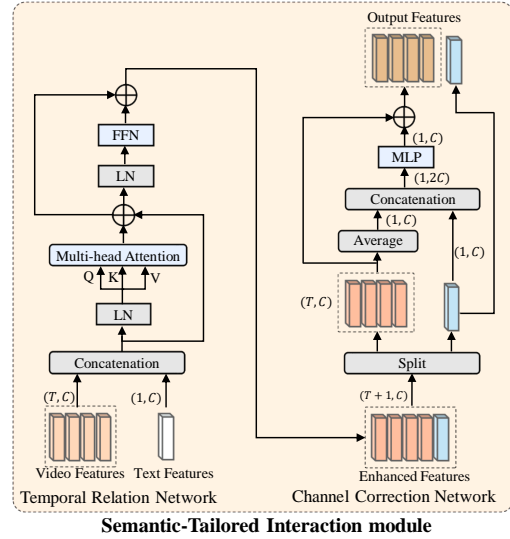


Fig. 3. Illustration of Semantic-Tailored Interaction (STI) module. STI consists of Temporal Relation Network and Channel Correction Network, which perform feature interaction in the temporal and channel domains, respectively.

capture temporal features from different velocity scales, where each temporal feature captures unique perspectives of temporal representations. In FSAR, with limited support videos, the learned velocity features tend to deviate from the underlying motion semantic without semantic information constraints. We argue that textual and visual information compensates for each other, and using linguistic prior knowledge promotes the visual features to pay more attention to semantic-related features. To this end, PSTI consists of multiple Semantic-Tailored Interaction blocks. Each block progressively utilizes the output text information of the last stage to enhance current semantic-related velocity features, and then each stage outputs corresponding velocity action features for velocity-aware matching.

As shown in Figure 3, the Semantic-Tailored Interaction block (STI) consists of two sub-networks: Temporal Relation Network and Channel Correction Network. These two networks compensate each other to inject semantic information into visual features, which allows the interaction between semantic information and visual features on the temporal and channel domains, respectively. Take an STI block as an example. In the STI block that processes information at the velocity scale n , the input visual features and textual features are $\mathbf{X}_{in}^n \in \mathbb{R}^{T \times C}$ and $\mathbf{q}_{in}^n \in \mathbb{R}^{1 \times C}$, respectively.

a) *Temporal Relation Network*:: Inspired by the prompt methods in NLP [62], we concatenate the visual features with the corresponding text feature, and feed them together into the Temporal Relation Network to obtain the enhanced features. Concretely, given the text feature $\mathbf{q}_{in}^n \in \mathbb{R}^{1 \times C}$ and the visual features $\mathbf{X}_{in}^n \in \mathbb{R}^{T \times C}$ at the velocity scale n , we obtain new sequence features $\hat{\mathbf{X}}^n$ by concatenating the text features and the visual features.

Then we feed the extended sequence features $\hat{\mathbf{X}}^n$ into the remaining transformer layers, which consist of layer normalization (LN), Multi-Headed Self-Attention (MSA), and MLP block to allow the interaction between the semantic token

and the visual tokens along the temporal dimension. Concretely, the interim interaction output $\hat{\mathbf{X}}^n$ is computed as

$$\dot{\mathbf{X}}^n = \hat{\mathbf{X}}^n + \text{MSA}(\hat{\mathbf{X}}^n), \quad (1)$$

$$\text{MSA}^h = \text{Softmax}\left(\frac{\mathbf{F}_q^h \mathbf{F}_k^{h\top}}{\sqrt{d}}\right) \mathbf{F}_v^h, \quad (2)$$

where MSA^h is a single attention head h in MSA , $\mathbf{F}_q^h = \text{LN}(\hat{\mathbf{X}}^n) \mathbf{W}_q^h$ is the query, $\mathbf{F}_k^h = \text{LN}(\hat{\mathbf{X}}^n) \mathbf{W}_k^h$ is the key, and $\mathbf{F}_v^h = \text{LN}(\hat{\mathbf{X}}^n) \mathbf{W}_v^h$ is the value. We concatenate all the attention heads and perform linear projection to obtain the final output $\dot{\mathbf{X}}^n$. Then, we further apply a feed-forward network to obtain enhanced feature $\bar{\mathbf{X}}^n$ as shown in Fig. 3, given by:

$$\bar{\mathbf{X}}^n = \dot{\mathbf{X}}^n + \text{FFN}(\text{LN}(\dot{\mathbf{X}}^n)), \quad (3)$$

where FFN is composed of two linear projections that are separated by a GELU non-linearity. The feature dimension stays unchanged.

b) Channel Correction Network: In addition to taking full account of temporal interaction between the visual features and the text semantic, we believe that taking advantage of text semantic information to perform channel interaction is conducive to multi-velocity feature construction. Thus, we propose a Channel Correction Network that utilizes the channel interaction to correct feature channels and enhance semantic-related velocity features. Specifically, given enhanced visual features $\bar{\mathbf{X}}^n = [\mathbf{x}_1, \mathbf{x}_2, \dots, \mathbf{x}_T]$, we first obtain a global visual context vector $\bar{\mathbf{x}}_g^n$ by averaging all visual tokens:

$$\bar{\mathbf{x}}_g^n = \frac{1}{T} \sum_{t=1}^T \mathbf{x}_t. \quad (4)$$

Then, we concatenate the global visual context vector with enhanced text feature $\bar{\mathbf{q}}^n$. Specifically, we employ a two-layer MLP module to learn relation-aware channel features and obtain a modulating global vector $\mathbf{p}_g^n \in \mathbb{R}^{1 \times C}$:

$$\mathbf{p}_g^n = \text{MLP}([\bar{\mathbf{x}}_g^n; \bar{\mathbf{q}}^n]), \quad (5)$$

$$\text{MLP}(\cdot) = \text{FC}(\text{ReLU}(\text{FC}(\cdot))), \quad (6)$$

where $\text{MLP}(\cdot)$ represents the MLP layer consisting of two fully connected layers and a ReLU layer. Finally, we add the modulated global vector to all visual tokens so that it can tune the visual features at each channel. The final modulated visual features $\mathbf{X}_{\text{out}}^n \in \mathbb{R}^{T \times C}$ can be written as:

$$\mathbf{X}_{\text{out}}^n = [\mathbf{x}_t + \mathbf{p}_g^n], t = 1, 2, \dots, T. \quad (7)$$

In addition, in order to preserve high-level scene information, we design a progressive connection operation to connect the visual outputs of the STI block at different velocity scales and pool features from the raw video input \mathbf{X}_{in}^n . Given the interaction feature output $\mathbf{X}_{\text{out}}^n \in \mathbb{R}^{T \times C}$, the progressive connection uses temporal fusion to provide $\mathbf{X}_{\text{in}}^{n+1} \in \mathbb{R}^{\frac{T}{2} \times C}$ for the next block, as follows,

$$\mathbf{X}_{\text{in}}^{n+1} = \text{Linear}(\text{TM}(\mathbf{X}_{\text{out}}^n) + \mathbf{X}_{\text{d}}^n), \quad (8)$$

$$\mathbf{X}_{\text{d}}^n = \text{Downsample}(\mathbf{X}_{\text{in}}^n), \quad (9)$$

where $\text{Downsample}(\cdot)$ is a weighted pooling operation among the neighboring tokens, and $\text{Linear}(\cdot)$ is a linear layer. $\text{TM}(\cdot)$ is a temporal merge block that uses a pooling operation to shrink the number of interaction feature tokens.

Similarly, we adopt the same operation on the query set videos to explore the temporal relationship. However, since the real class information of the query video is unknown during testing, we only input the visual query feature into the Semantic-Tailor Interaction block. For the whole PSTI module, we repeat the above process to recurrently inject velocity-tailored text information and progressively interact with video-text information at different velocity levels.

D. Multi-Velocity Feature Alignment

Given the substantial variations in motion speed among action instances, it becomes possible to simultaneously perform multi-velocity feature matching for each specific action. As mentioned in the above section, we acquire multiple velocity representations, with each carrying distinct velocity information. Consequently, we propose a Multi-Velocity Feature Alignment (MVFA) module to capture pair-wise semantic relevance at different velocity levels, thereby facilitating coherent matching between videos.

Specifically, given different velocity action feature outputs from the PSTI module, the proposed MVFA module calculates the query-support distance at each velocity level and then obtains the overall query-support distance by the weighted sum of the distances. Specifically, given the support visual feature outputs $\bar{\mathbf{X}}_s^n = [\bar{\mathbf{x}}_s^{n1}, \dots, \bar{\mathbf{x}}_s^{n2^{4-n}}]$ and the query visual features $\bar{\mathbf{X}}_q^n = [\bar{\mathbf{x}}_q^{n1}, \dots, \bar{\mathbf{x}}_q^{n2^{4-n}}]$ at velocity scale n , we adopt the temporal alignment metric on these features:

$$D(\bar{\mathbf{X}}_s^n, \bar{\mathbf{X}}_q^n) = \mathcal{M}([\bar{\mathbf{x}}_s^{n1}, \dots, \bar{\mathbf{x}}_s^{n2^{4-n}}], [\bar{\mathbf{x}}_q^{n1}, \dots, \bar{\mathbf{x}}_q^{n2^{4-n}}]), \quad (10)$$

where $D(\bar{\mathbf{X}}_s^n, \bar{\mathbf{X}}_q^n)$ is the distance between the support visual feature $\bar{\mathbf{X}}_s^n$ and the query visual feature $\bar{\mathbf{X}}_q^n$. \mathcal{M} is the OTAM metric [11] by default in our MVP-Shot. Note that the proposed MVP-Shot is a plug-and-play framework and in the later experimental section, we will insert MVP-Shot into other existing metrics or methods and empirically demonstrate its pluggability. Furthermore, we express the total support-query distance between support and query videos as the weighted sum of the distances obtained by multiple velocity scales:

$$D_{s,q} = \sum_{n=1}^N \alpha_n D(\bar{\mathbf{X}}_s^n, \bar{\mathbf{X}}_q^n), \quad (11)$$

where α_n is the coefficient. By default, the maximum velocity scale N is set to 3 in this paper for considering the balance between effectiveness and efficiency.

To tackle the issue that different action instances may be performed at different motion dynamics, we propose PSTI and MVFA to progressively capture and align multi-velocity action features. By this means, our proposed MVP-shot combines two modules to complement each other to predict query categories more accurately under the few-shot setting.

Finally, we can use the output total support-query distance $D_{s,q}$ as logits for classification. Following previous works, we can use a cross-entropy loss \mathcal{L}_{CE} to optimize the model

TABLE I

COMPARISON WITH RECENT STATE-OF-THE-ART FEW-SHOT ACTION RECOGNITION METHODS (§IV-C) ON KINETICS [21], UCF101 [20] AND HMDB51 [19]. THE EXPERIMENT SETTINGS ARE CONDUCTED UNDER THE 5-WAY K -SHOT. "INET-RN50" DENOTES RESNET-50 PRE-TRAINED ON IMAGENET"--" MEANS THE RESULT IS NOT AVAILABLE IN PUBLISHED WORKS. THE BEST RESULTS ARE HIGHLIGHTED.

Method	Pre-training	Kinetics			UCF101			HMDB51		
		1-shot (%)	3-shot (%)	5-shot (%)	1-shot (%)	3-shot (%)	5-shot (%)	1-shot (%)	3-shot (%)	5-shot (%)
MatchingNet [61] ^[NeurIPS16]	INet-RN50	53.3	69.2	74.6	-	-	-	-	-	-
CMN [6] ^[ECCV18]	INet-RN50	57.3	75.6	76.0	-	-	-	-	-	-
ARN [17] ^[ECCV20]	INet-RN50	63.7	-	82.4	66.3	-	83.1	45.5	-	60.6
OTAM [11] ^[CVPR20]	INet-RN50	73.0	78.7	85.8	79.9	87.0	-	54.5	65.7	-
ITANet [44] ^[IJCAI21]	INet-RN50	73.6	-	84.3	-	-	-	-	-	-
TRX [14] ^[CVPR21]	INet-RN50	63.6	81.8	85.9	78.2	92.4	96.1	53.1	66.8	75.6
TA ² N [12] ^[AAAI22]	INet-RN50	72.8	-	85.8	81.9	-	95.9	59.7	-	73.9
MTFAN [41] ^[CVPR22]	INet-RN50	74.6	-	87.4	84.8	-	95.1	59.0	-	74.6
HyRSM [7] ^[CVPR22]	INet-RN50	73.7	83.5	86.1	83.9	93.0	94.7	60.3	71.7	76.0
STRM [13] ^[CVPR22]	INet-RN50	62.9	81.1	86.7	80.5	92.7	96.9	52.3	67.4	77.3
CPM [8] ^[ECCV22]	INet-RN50	73.3	-	-	71.4	-	-	60.1	-	-
HCL [63] ^[ECCV22]	INet-RN50	73.7	82.4	85.8	82.6	91.0	94.5	59.1	71.2	76.3
MoLo [64] ^[CVPR23]	INet-RN50	74.0	83.7	85.6	86.0	93.5	95.5	60.8	72.0	77.4
GgHM [9] ^[ICCV23]	INet-RN50	74.9	-	87.4	85.2	-	96.3	61.2	-	76.9
CLIP-Freeze [56] ^[ICML21]	CLIP-RN50	68.2	82.1	85.3	84.6	92.9	94.5	51.4	65.2	71.0
CLIP-FSAR [60] ^[IJCV23]	CLIP-RN50	87.6	90.7	91.9	91.3	95.1	97.0	69.2	77.6	80.3
MVP-shot (Ours)	CLIP-RN50	90.0	92.0	93.2	92.2	96.9	97.6	72.5	79.7	82.5

TABLE II

COMPARISON WITH RECENT STATE-OF-THE-ART FEW-SHOT ACTION RECOGNITION METHODS (§IV-C) ON SSV2-SMALL [22] DATASET. THE EXPERIMENT SETTINGS ARE CONDUCTED UNDER THE 5-WAY K -SHOT. "INET-RN50" DENOTES RESNET-50 PRE-TRAINED ON IMAGENET"--" MEANS THE RESULT IS NOT AVAILABLE IN PUBLISHED WORKS. THE BEST RESULTS ARE HIGHLIGHTED.

Method	Pre-training	SSv2-small		
		1-shot (%)	3-shot (%)	5-shot (%)
MatchingNet [61] ^[NeurIPS16]	INet-RN50	31.3	39.8	45.5
MAML [26] ^[ICML17]	INet-RN50	30.9	38.6	41.9
CMN [6] ^[ECCV18]	INet-RN50	36.2	42.5	48.8
OTAM [11] ^[CVPR20]	INet-RN50	36.4	45.9	48.0
ITANet [44] ^[IJCAI21]	INet-RN50	39.8	49.4	53.7
TRX [14] ^[CVPR21]	INet-RN50	36.0	51.9	56.7
HyRSM [7] ^[CVPR22]	INet-RN50	40.6	-	56.1
STRM [13] ^[CVPR22]	INet-RN50	37.1	49.2	55.3
HCL [63] ^[ECCV22]	INet-RN50	38.9	49.1	55.4
MoLo [64] ^[CVPR23]	INet-RN50	42.7	50.9	56.4
CLIP-Freeze [56] ^[ICML21]	CLIP-RN50	26.8	33.7	36.3
CLIP-FSAR [60] ^[IJCV23]	CLIP-RN50	52.0	54.0	55.8
MVP-shot (Ours)	CLIP-RN50	51.2	55.2	57.0

parameters. For few-shot inference, we can leverage the distance values of support-query video pairs in (11) to classify query samples based on the nearest neighbor rule [39].

IV. EXPERIMENTS

In this section, we first describe four few-shot action recognition datasets (i.e., Kinetics [21], UCF101 [20], HMDB51 [19], and SSV2-small [22]) and the evaluation protocol (§IV-A). Then we introduce the implementation Details of our MVP-shot (§IV-B). After that, we compare our methods with previous state-of-the-art few-shot action recognition methods on four

gold-standard datasets (§IV-C). Finally, we perform several ablation experiments to demonstrate the effectiveness of the proposed MVP-shot (§IV-D).

A. Experimental Setup

Dataset. We evaluate the effectiveness of our proposed method on four benchmarks, i.e., Kinetics [21], SSV2-small [22], UCF101 [20], and HMDB51 [19], using 5-way 1/3/5-shot few-shot recognition tasks for all models considered. For Kinetics and SSV2-small, we follow the split setting as in CMN [6], which both randomly select 64 classes from the original dataset as the train set, 12 classes as the val set and 24 classes as the test set. For HMDB51 [19], we use the splits from [17], and the dataset has 31 action classes, 10 action classes, and 10 action classes for train/val/test, respectively. The UCF101 [20] dataset contains 101 action classes, and we adopt the splits from [17], which splits the dataset into 70/10/21 classes for train/val/test, respectively.

Evaluation. Following the official evaluation protocols [9], [11], we use 5-way 1-shot and 5-way 5-shot accuracy for evaluation, and report average results over 10,000 tasks randomly selected from test.

B. Implementation Details

Network Architecture. For a fair comparison with previous works [11], [14] that use Resnet-50 [65] pre-trained on ImageNet [66] as the backbone, we provide a version of utilizing pre-trained CLIP ResNet-50 as our basic visual encoder. To retain the original pre-trained prior knowledge in the text encoder and reduce the optimization burden, we freeze the text encoder and prevent it from being updated during training.

TABLE III

ABLATION STUDY OF EACH COMPONENT IN OUR MVP-SHOT (§IV-D). WE REPORTED THE 1-SHOT AND 5-SHOT RESULTS ON KINETICS [21] DATASET. THE BEST RESULTS ARE HIGHLIGHTED.

PSTI	MVFA	Kinetics	
		1-shot (%)	5-shot (%)
\times	\times	79.8	89.3
\checkmark	\times	88.3	92.3
\times	\checkmark	81.9	91.8
\checkmark	\checkmark	90.0	93.2

Network Training. Following previous methods [67], we sparsely and uniformly sample $T = 8$ frames to obtain the representation of the whole video. Each frame is scaled to a height of 256. Each video frame is first resized to 256×256 , and then these resized video frames are randomly cropped into the size of 224×224 . In the training phase, we adopt basic data augmentation, such as random horizontal flipping, cropping, and color jitter. Moreover, our framework uses the Adam optimizer with the multi-step scheduler to train our model. The total number of training steps is set to 10. In the inference phase, we report the mean video classification accuracy in 10000 episodes randomly sampled from the test sets. For many shot classifications, we follow the prototype paradigm [39] and calculate the mean features of support videos in each class as the prototypes to classify query videos. **Reproducibility.** Our model is implemented in PyTorch and trained on two TITAN RTX GPUs with a 24GB memory per-card. Testing is conducted on the same machine. To guarantee reproducibility, full code will be released.

C. Comparison with SOTA methods

Results on Kinetics [21], HMDB51 [19] and UCF101 [20].

Table I demonstrates our method outperforms other state-of-the-art methods on Kinetics, UCF101, and HMDB51 datasets under the 1-shot to 5-shot setting. Table I demonstrates our method outperforms other state-of-the-art methods on Kinetics, UCF101, and HMDB51 datasets under the 1-shot to 5-shot setting. Specifically, our model significantly improves accuracy in any task setting compared to previous excellent methods (such as TRX [14], HyRSM [7], and MoLo [64]). Compared to CLIP-FSAR [60], which uses the same CLIP pre-training and temporal alignment metric, our MVP-shot achieves better results in multiple datasets and task settings. Notably, compared to CLIP-FSAR [60], our method brings 3.3%, 2.4% performance improvements in the 1-shot task of HMDB51 and Kinetics, and 2.2%, 1.3% gains in the 5-shot task of HMDB51 and Kinetics, respectively.

Results on SSV2-small [22]. We also report our MVP-shot model results on SSV2-small datasets on Table II. Our CLIP-RN50 model achieves the best performance in the 3-shot and 5-shot tasks compared to all the methods using ResNet-50 as the visual encoder. Compared to CLIP-FSAR [60], our method also has a significant performance improvement. Concretely, our MVP-shot brings 1.0% accuracy improvements in the 3-shot task, and 1.2% accuracy gains in the 5-shot task, respectively.

TABLE IV

ABLATION STUDY OF VELOCITY SCALES IN MULTI-VELOCITY FEATURE ALIGNMENT IN OUR MVP-SHOT (§IV-D). WE REPORTED THE 1-SHOT AND 5-SHOT RESULTS ON KINETICS [21] DATASET. THE BEST RESULTS ARE HIGHLIGHTED.

Velocity			Kinetics	
$n = 1$	$n = 2$	$n = 3$	1-shot (%)	5-shot (%)
\times	\times	\checkmark	81.6	87.0
\times	\checkmark	\times	86.0	90.5
\checkmark	\times	\times	88.3	92.3
\times	\checkmark	\checkmark	81.9	91.8
\checkmark	\times	\checkmark	88.8	92.5
\checkmark	\checkmark	\times	89.5	93.0
\checkmark	\checkmark	\checkmark	90.0	93.2

Excellent performance on these datasets reveals that our MVP-shot has strong robustness and generalization for different datasets. In addition, from the experimental results, we can make the following observations. (1) Compared with CLIP-FSAR [60] using the same CLIP pre-training and temporal alignment metric, our MVP-shot achieves better results in multiple datasets and task settings. Specifically, MVP-shot brings 3.3% and 2.4% performance improvements in the 1-shot tasks of HMDB51 and Kinetics, respectively. It indicates our MVP-shot further boosts performance by exploring multi-velocity feature matching. (2) We observe that MVP-shot outperforms current state-of-the-art methods (such as TRX [14], HyRSM [7], and MoLo [64]), especially under the 1-shot and 3-shot settings. We attribute this to the fact that introducing text semantic cues would be more effective for enhancing semantic-related velocity features when visual information is insufficient.

D. Ablation Study

We conduct ablation experiments to validate the capability of the proposed MVP-shot and analyze the contribution of each component. Unless otherwise specified, we adopt the CLIP-RN50 model as the default visual encoder.

Analysis of Each Module in MVP-shot. To validate the contributions of each module in our method, we conduct experiments under 5-way 1-shot and 5-shot settings on the Kinetics [21] datasets. Table III summarizes the effects of each module in MVP-shot. By performing multi-velocity feature alignment (MVFA) (*c.f.* §III-C), we obtain 2.1% and 2.5% 1-shot and 5-shot improvements, respectively. This consistent promotion indicates that MVFA can capture pair-wise semantic relevance at different velocity scales to facilitate accurate matching between videos. In addition, the proposed Progressive Semantic-Tailored Interaction (PSTI) module (*c.f.* §III-D) improves on 1-shot and 5-shot by 8.5% and 3.0%, respectively, which indicates recurrently injecting velocity-tailored text information significantly boosts performance. We observe that the performance gain is particularly significant in the 1-shot scenario, suggesting that it would be more effective to supplement textual semantic information when visual information is

TABLE V
COMPARISON OF DIFFERENT FEATURE INTERACTION METHODS (§IV-D).
WE REPORTED THE 1-SHOT AND 5-SHOT RESULTS ON KINETICS [21]
DATASET. THE BEST RESULTS ARE HIGHLIGHTED.

Method	Kinetics	
	1-shot (%)	5-shot (%)
Single-modal Transformer	81.5	92.0
Multi-modal Transformer	88.9	92.7
STI (ours)	90.0	93.2

TABLE VI
GENERALIZATION PERFORMANCE OF MVP-SHOT WITH DIFFERENT
TEMPORAL ALIGNMENT METRICS (§IV-D) ON KINETICS [21] IN THE 5-WAY
1-SHOT AND 5-WAY 5-SHOT TASKS.

Method	Kinetics	
	1-shot (%)	5-shot (%)
Bi-MHM [7]	81.5	91.6
CLIP-FSAR (Bi-MHM)	87.7	92.1
Ours (Bi-MHM)	89.4	92.9
OTAM [11]	81.9	91.8
CLIP-FSAR (OTAM)	87.6	91.9
Ours (OTAM)	90.0	93.2

very limited. Moreover, stacking MVFA and PSTI modules can further improve performance, indicating the complementarity between components.

Analysis of Multi-Velocity Feature Alignment. To demonstrate that multi-velocity feature alignment coordinates with each other to facilitate accurate matching between videos, we conduct the experiments on the 5-way 1-shot and 5-shot tasks of Kinetics [21] by various combinations of multi-velocity feature alignment. The obtained results are reported in Table IV. When the action feature is provided at a single velocity, the corresponding performance is reduced on the 1-shot and 5-shot settings. The performance of multi-velocity feature alignment improves as the velocity scales increase. Further, our MVP-shot, which combines all velocity feature alignments, achieves the best performance. Specifically, on the 1-shot setting, MVP-shot outperforms all single-velocity feature alignments by 1.7%, 4.0%, and 8.4%, respectively. These results demonstrate that our proposed multi-velocity feature alignment can surpass corresponding methods with single-velocity feature alignment, and capture pair-wise semantic relevance at different velocity scales to facilitate coherent matching between videos.

Comparison with Different Feature Interaction Methods. To demonstrate the effectiveness of our proposed Semantic-Tailored Interaction (STI) module and compare the efficacy of various feature interaction methods, we conduct experiments on the 5-way 1-shot and 5-way 5-shot task of Kinetics [21]. Specifically, we replace our STI module with several other feature interaction methods. The transformer [68] consists of the multi-head self-attention and a feed-forward network. The first baseline single-modal transformer indicates the support features and query features doing self-attention on the temporal dimension without text features. Compared with the first baseline, the second multi-modal transformer (CLIP-FSAR [60]) stacks the text features to the corresponding

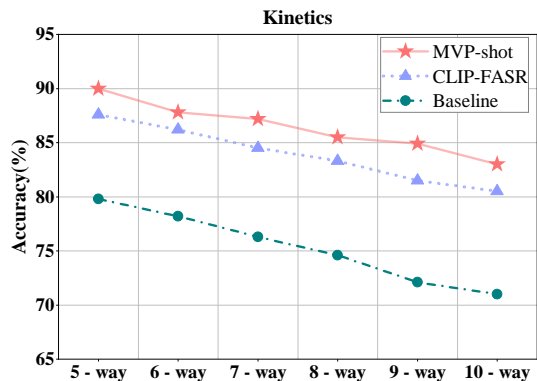


Fig. 4. N -way 1-shot results of our MVP-shot on Kinetics [21] dataset, CLIP-FSAR and our baseline methods with N varying from 5 to 10.

support features along the temporal dimension before self-attention. We set all the layers of the transformer to be one. For a fair comparison, the other experimental settings are the same as the proposed MVP-shot. The experimental results are shown in Table V. In comparison, the proposed STI module outperforms the unimodal transformer by 8.5% (90.0% vs. 81.5%) and 1.2% (93.2% vs. 92.0%) on the 1-shot and 5-shot settings, respectively. The performance gains indicate that there is complementarity between visual and textual modalities, and semantic information can help visual features to be more discriminative. Compared with the multimodal transformer, the proposed STI module increases 1.7% (88.3% vs. 90.0%) and 0.9% (92.3% vs. 93.2%) on the 1-shot and 5-shot settings, respectively. Experimental results demonstrate that STI module enhances the utilization of textual information more efficiently to capture the semantic-related velocity features. Thus, our proposed module can achieve more robust and more accurate class prototype estimation.

Generalization on Different Alignment Metrics. We conduct the experiments using different temporal alignment metrics on the 5-way 1-shot and 5-way 5-shot tasks of Kinetics [21] to demonstrate our model generalizability. We adopt different temporal alignment metrics, including OTAM [11] and Bi-MHM [7]. As shown in Table VI, our method can adapt to any temporal alignment metric, and achieve great performance. Moreover, irrespective of the temporal alignment metric employed, our framework still achieves impressive performance gains compared to the naive baselines, indicating the superiority of our method.

Influence of different backbones. The previous comparison results are all based on CLIP-RN50. Here, we conduct detailed experiments to evaluate the impact of different backbones. We adopt the CLIP-ViT-B backbone, and the other settings are the same as those of our work. We list comparison results with CLIP-FSAR based on the CLIP-ViT-B backbone in Table VII. We conduct the experiments on four gold-standard datasets (*i.e.*, HMDB51 [19], UCF101 [20], kinetics100 [21], and SSV2-small [22]). From Table VII, we can see our MVP-shot based on CLIP-ViT-B consistently outperforms CLIP-FSAR [60], demonstrating the effectiveness of our method. In addition, MVP-shot based on CLIP-ViT-B generally achieves results superior to that based on CLIP-RN50, suggesting that

TABLE VII

INFLUENCE OF DIFFERENT BACKBONES. QUANTITATIVE COMPARISON RESULTS (§IV-D) ON KINETICS [21], UCF101 [20], HMDB51 [19], AND SSV2-SMALL [22]. “-” MEANS THE RESULT IS NOT AVAILABLE IN PUBLISHED WORKS. THE BEST RESULTS ARE HIGHLIGHTED.

Method	Pre-training	Kinetics		UCF101		HMDB51		SSv2-small	
		1-shot (%)	5-shot (%)	1-shot (%)	5-shot (%)	1-shot (%)	5-shot (%)	1-shot (%)	5-shot (%)
CLIP-FSAR	CLIP-RN50	87.6	91.9	91.3	97.0	69.2	80.3	52.0	55.8
MVP-shot (Ours)		90.0	93.2	92.2	97.6	72.5	82.5	51.2	57.0
CLIP-FSAR	CLIP-ViT-B	89.7	95.0	96.6	99.0	75.8	87.7	54.5	61.8
MVP-shot (Ours)		91.0	95.1	96.8	99.0	77.0	88.1	55.4	62.0

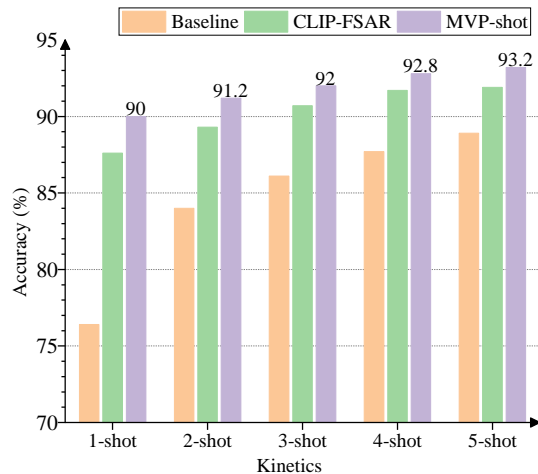


Fig. 5. Comparison results (§IV-D) with different numbers of support samples in 5-way K -shot setting on kinetics [21] dataset.

a stronger pre-trained model contributes to enhanced few-shot generalization.

Testing of N -Way Few-Shot Action Recognition. In the previous experiments, all of our comparative evaluation experiments are carried out under the 5-way setting. To further explore the effect of varying N on the few-shot performance, we compare N -way 1-shot results on Kinetics in Fig. 4, where N varies from 5 to 10. Results show as N increases, the classification difficulty becomes higher. For example, the 10-way result of MVP-shot decreases by 7.0% compared to the 5-way result. Nevertheless, the performance of our MVP-shot is still consistently ahead of the comparison methods, such as CLIP-FSAR [60]. This demonstrated that our proposed MVP-shot can boost performance by jointly exploring multi-velocity feature representation and multi-velocity feature alignment.

5-way K -shot Few-shot Classification. To more comprehensively assess the performance of our model in various few-shot scenarios, we conduct extra experiments on Kinetics [21] by increasing the number of support samples from 1-shot to 5-shot. As shown in Fig. 5, as K decreases, the classification difficulty becomes higher, and the performance decreases. Though too few support samples limit the performance of MVP-shot and CLIP-FSAR [60], MVP-shot performs consistently better than baseline and CLIP-FSAR in all settings. This demonstrates that our proposed MVP-shot can boost performance by exploring multi-velocity feature matching.

E. Visualization Analysis

Similarity Visualization. To qualitatively demonstrate the proposed multi-velocity feature alignment in our method, we visualize the predicted similarities between query and support prototypes for an episode under both single-velocity and multi-velocity settings in Fig. 6. Compared to single-velocity alignment, multi-velocity alignment captures pair-wise semantic relevance at different velocity scales, compensating for the shortcomings of single-velocity alignment. Thus, our proposed multi-velocity alignment makes more accurate decisions. Specifically, for the fourth query sample in Kinetics, the incorrect decision obtained by the single-velocity ($n=1$) matching can be rectified by fusing the results of multi-velocity matching. Experimental results demonstrate that multi-velocity matching complements each other, and combines alignment across all velocity features, achieving the best performance.

Attention Visualization of Our MVP-shot. Fig. 7 shows the attention visualization of our MVP-shot on UCF101 [20] and HMDB51 [19] in the 5-way 1-shot setting. according to the input RGB image sequences, the attention maps of the multi-modal transformer model using CLIP pre-trained weights, which we have mentioned in §IV-D, are compared to the attention maps with our MVP-shot, which refers to Progressive Semantic-Tailored Interaction module (PSTI). The attention map generated with multi-modal transformer often contains a significant number of unrelated or distracting focus areas. In contrast, the attention maps generated by our MVP-shot, which uses the PSTI module, focus more on action-related objects and reduce attention to the background and unrelated objects. Specifically, the frames in “Ride Horse” focus on the person on the horse, and the frames in “Ice Dancing” focus on dancers on the ice. These observations provide empirical evidence of the effectiveness of our PSTI module in enhancing semantic and spatiotemporal representation.

V. CONCLUSION

In this work, we first point out that single-scale feature alignment in previous FSAR methods is insufficient to reflect the speed diversity of action instances. To alleviate this problem, we propose a novel MVP-shot framework to obtain and align multi-velocity action features in a progressive way. A Progressive Semantic-Tailored Interaction module is designed to capture trustworthy multi-velocity feature representation. Subsequently, a Multi-Velocity Feature Alignment module is presented to measure the similarity of multi-velocity action features. By

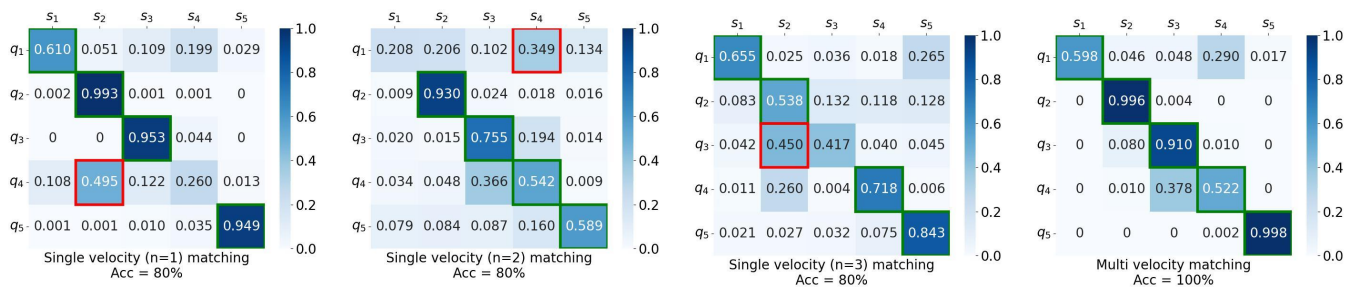


Fig. 6. Similarity visualization between query samples (q_n) and support prototypes (s_n) with different methods in a meta-test episode from Kinetics. The action classes, from left to right, are *Shot Put*, *Catching or Throwing Baseball*, *Playing Ice Hockey*, *Drop Kicking* and *Dribbling Basketball*, respectively. A higher score indicates a greater degree of similarity. The green box indicates correct prediction and the red box indicates incorrect prediction.

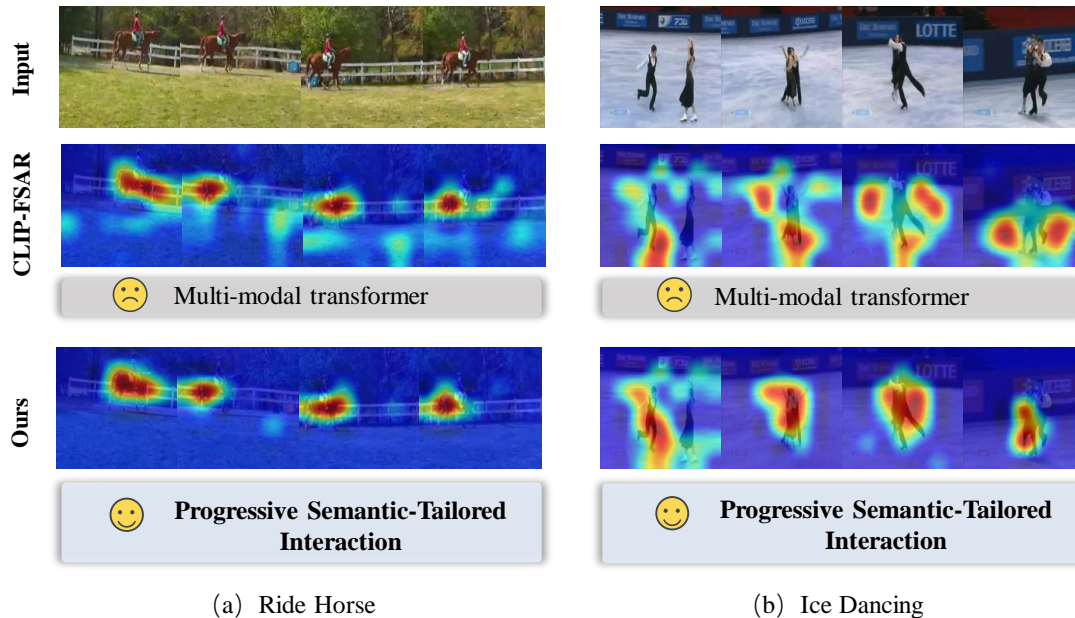


Fig. 7. Attention visualization of our MVP-shot on HMDB51 [19] and UCF101 [20] in the 5-way 1-shot setting. Corresponding to the original RGB images (left), the attention maps of the multi-modal transformer model (middle) are compared to the attention maps of our MVP-shot (right). The temporal alignment metric is OTAM [11].

this means, our MVP-shot enables robust and comprehensive few-shot matching. Experimental results demonstrate that MVP-shot achieves state-of-the-art performance on the four standard benchmarks.

However, this is the first cursory exploration of achieving multi-velocity feature matching in FSAR. Though the first step is always not elegant, more attempts and tricks in terms of multi-velocity features will be interesting in the future.

REFERENCES

- [1] C. Feichtenhofer, H. Fan, J. Malik, and K. He, “Slowfast networks for video recognition,” in *ICCV*, 2019, pp. 6202–6211.
- [2] J. Lin, C. Gan, and S. Han, “Tsm: Temporal shift module for efficient video understanding,” in *ICCV*, 2019, pp. 7083–7093.
- [3] Z. Qing, S. Zhang, Z. Huang, X. Wang, Y. Wang, Y. Lv, C. Gao, and N. Sang, “Mar: Masked autoencoders for efficient action recognition,” *IEEE Transactions on Multimedia*, 2023.
- [4] M. Wang, X. Li, S. Chen, X. Zhang, L. Ma, and Y. Zhang, “Learning representations by contrastive spatio-temporal clustering for skeleton-based action recognition,” *IEEE Transactions on Multimedia*, 2023.
- [5] P. Huang, R. Yan, X. Shu, Z. Tu, G. Dai, and J. Tang, “Semantic-disentangled transformer with noun-verb embedding for compositional action recognition,” *IEEE Transactions on Image Processing*, 2023.
- [6] L. Zhu and Y. Yang, “Compound memory networks for few-shot video classification,” in *ECCV*, 2018, pp. 751–766.
- [7] X. Wang, S. Zhang, Z. Qing, M. Tang, Z. Zuo, C. Gao, R. Jin, and N. Sang, “Hybrid relation guided set matching for few-shot action recognition,” in *CVPR*, 2022, pp. 19948–19957.
- [8] Y. Huang, L. Yang, and Y. Sato, “Compound prototype matching for few-shot action recognition,” in *ECCV*, 2022, pp. 351–368.
- [9] J. Xing, M. Wang, Y. Ruan, B. Chen, Y. Guo, B. Mu, G. Dai, J. Wang, and Y. Liu, “Boosting few-shot action recognition with graph-guided hybrid matching,” in *ICCV*, 2023, pp. 1740–1750.
- [10] Y. Shi, X. Wu, H. Lin, and J. Luo, “Commonsense knowledge prompting for few-shot action recognition in videos,” *IEEE Transactions on Multimedia*, 2024.
- [11] K. Cao, J. Ji, Z. Cao, C.-Y. Chang, and J. C. Niebles, “Few-shot video classification via temporal alignment,” in *CVPR*, 2020, pp. 10 618–10 627.
- [12] S. Li, H. Liu, R. Qian, Y. Li, J. See, M. Fei, X. Yu, and W. Lin, “Ta2n: Two-stage action alignment network for few-shot action recognition,” in *AAAI*, vol. 36, no. 2, 2022, pp. 1404–1411.
- [13] A. Thatipelli, S. Narayan, S. Khan, R. M. Anwer, F. S. Khan, and B. Ghanem, “Spatio-temporal relation modeling for few-shot action recognition,” in *CVPR*, 2022, pp. 19958–19967.
- [14] T. Perrett, A. Masullo, T. Burghardt, M. Mirmehdi, and D. Damen, “Temporal-relational crosstransformers for few-shot action recognition,” in *CVPR*, 2021, pp. 475–484.
- [15] M. Bishay, G. Zoumpourlis, and I. Patras, “Tarn: Temporal attentive relation network for few-shot and zero-shot action recognition,” in *BMVC*,

- 2019.
- [16] R. Ben-Ari, M. S. Nacson, O. Azulai, U. Barzelay, and D. Rotman, "Taen: temporal aware embedding network for few-shot action recognition," in *CVPR*, 2021, pp. 2786–2794.
- [17] H. Zhang, L. Zhang, X. Qi, H. Li, P. H. Torr, and P. Koniusz, "Few-shot action recognition with permutation-invariant attention," in *ECCV*, 2020, pp. 525–542.
- [18] M. Maier and R. Abdel Rahman, "No matter how: Top-down effects of verbal and semantic category knowledge on early visual perception," *Cognitive, Affective, & Behavioral Neuroscience*, vol. 19, pp. 859–876, 2019.
- [19] H. Kuehne, H. Jhuang, E. Garrote, T. Poggio, and T. Serre, "Hmdb: a large video database for human motion recognition," in *ICCV*, 2011, pp. 2556–2563.
- [20] K. Soomro, A. R. Zamir, and M. Shah, "Ucf101: A dataset of 101 human actions classes from videos in the wild," *arXiv preprint arXiv:1212.0402*, 2012.
- [21] J. Carreira and A. Zisserman, "Quo vadis, action recognition? a new model and the kinetics dataset," in *CVPR*, 2017, pp. 6299–6308.
- [22] R. Goyal, S. Ebrahimi Kahou, V. Michalski, J. Materzynska, S. Westphal, H. Kim, V. Haenel, I. Friend, P. Yianilos, M. Mueller-Freitag *et al.*, "The" something something" video database for learning and evaluating visual common sense," in *ICCV*, 2017, pp. 5842–5850.
- [23] Z. Chen, Y. Fu, Y.-X. Wang, L. Ma, W. Liu, and M. Hebert, "Image deformation meta-networks for one-shot learning," in *CVPR*, 2019, pp. 8680–8689.
- [24] K. Li, Y. Zhang, K. Li, and Y. Fu, "Adversarial feature hallucination networks for few-shot learning," in *CVPR*, 2020, pp. 13 470–13 479.
- [25] H.-J. Ye, H. Hu, and D.-C. Zhan, "Learning adaptive classifiers synthesis for generalized few-shot learning," *International Journal of Computer Vision*, vol. 129, pp. 1930–1953, 2021.
- [26] C. Finn, P. Abbeel, and S. Levine, "Model-agnostic meta-learning for fast adaptation of deep networks," in *ICML*, 2017, pp. 1126–1135.
- [27] M. A. Jamal and G.-J. Qi, "Task agnostic meta-learning for few-shot learning," in *CVPR*, 2019, pp. 11 719–11 727.
- [28] A. Rajeswaran, C. Finn, S. M. Kakade, and S. Levine, "Meta-learning with implicit gradients," in *NIPS*, vol. 32, 2019.
- [29] A. A. Rusu, D. Rao, J. Sygnowski, O. Vinyals, R. Pascanu, S. Osindero, and R. Hadsell, "Meta-learning with latent embedding optimization," in *ICLR*, 2018.
- [30] Y. Wang, W.-L. Chao, K. Q. Weinberger, and L. Van Der Maaten, "Simpleshot: Revisiting nearest-neighbor classification for few-shot learning," *arXiv preprint arXiv:1911.04623*, 2019.
- [31] H.-J. Ye, H. Hu, D.-C. Zhan, and F. Sha, "Few-shot learning via embedding adaptation with set-to-set functions," in *CVPR*, 2020, pp. 8808–8817.
- [32] W. Chen, C. Si, Z. Zhang, L. Wang, Z. Wang, and T. Tan, "Semantic prompt for few-shot image recognition," in *CVPR*, 2023, pp. 23 581–23 591.
- [33] M. Han, Y. Zhan, Y. Luo, H. Hu, K. Su, and B. Du, "Textual enhanced adaptive meta-fusion for few-shot visual recognition," *IEEE Transactions on Multimedia*, 2023.
- [34] F. Peng, X. Yang, L. Xiao, Y. Wang, and C. Xu, "Sgva-clip: Semantic-guided visual adapting of vision-language models for few-shot image classification," *IEEE Transactions on Multimedia*, 2023.
- [35] X. Zhong, C. Gu, M. Ye, W. Huang, and C.-W. Lin, "Graph complemented latent representation for few-shot image classification," *IEEE Transactions on Multimedia*, 2022.
- [36] H. Cheng, J. T. Zhou, W. P. Tay, and B. Wen, "Graph neural networks with triple attention for few-shot learning," *IEEE Transactions on Multimedia*, 2023.
- [37] S. W. Yoon, J. Seo, and J. Moon, "Tapnet: Neural network augmented with task-adaptive projection for few-shot learning," in *ICML*, 2019, pp. 7115–7123.
- [38] S. Qiao, C. Liu, W. Shen, and A. L. Yuille, "Few-shot image recognition by predicting parameters from activations," in *CVPR*, 2018, pp. 7229–7238.
- [39] J. Snell, K. Swersky, and R. Zemel, "Prototypical networks for few-shot learning," in *NIPS*, vol. 30, 2017.
- [40] B. Liu, T. Zheng, P. Zheng, D. Liu, X. Qu, J. Gao, J. Dong, and X. Wang, "Lite-mkd: A multi-modal knowledge distillation framework for lightweight few-shot action recognition," in *ACM MM*, 2023, pp. 7283–7294.
- [41] J. Wu, T. Zhang, Z. Zhang, F. Wu, and Y. Zhang, "Motion-modulated temporal fragment alignment network for few-shot action recognition," in *CVPR*, 2022, pp. 9151–9160.
- [42] J. Xing, M. Wang, Y. Liu, and B. Mu, "Revisiting the spatial and temporal modeling for few-shot action recognition," in *AAAI*, vol. 37, no. 3, 2023, pp. 3001–3009.
- [43] H. Tang, J. Liu, S. Yan, R. Yan, Z. Li, and J. Tang, "M3net: Multi-view encoding, matching, and fusion for few-shot fine-grained action recognition," in *ACM MM*, 2023, pp. 1719–1728.
- [44] S. Zhang, J. Zhou, and X. He, "Learning implicit temporal alignment for few-shot video classification," in *IJCAI*, 2021.
- [45] Y. Cao, X. Su, Q. Tang, S. You, X. Lu, and C. Xu, "Searching for better spatio-temporal alignment in few-shot action recognition," *NIPS*, vol. 35, pp. 21 429–21 441, 2022.
- [46] C. Li, J. Zhang, S. Wu, X. Jin, and S. Shan, "Hierarchical compositional representations for few-shot action recognition," *Computer Vision and Image Understanding*, p. 103911, 2024.
- [47] J. Tang, X. Shu, G.-J. Qi, Z. Li, M. Wang, S. Yan, and R. Jain, "Tri-clustered tensor completion for social-aware image tag refinement," *IEEE transactions on pattern analysis and machine intelligence*, vol. 39, no. 8, pp. 1662–1674, 2016.
- [48] X. Shu, G.-J. Qi, J. Tang, and J. Wang, "Weakly-shared deep transfer networks for heterogeneous-domain knowledge propagation," in *Proceedings of the 23rd ACM international conference on Multimedia*, 2015, pp. 35–44.
- [49] X. Shu, J. Tang, G.-J. Qi, W. Liu, and J. Yang, "Hierarchical long short-term concurrent memory for human interaction recognition," *IEEE transactions on pattern analysis and machine intelligence*, vol. 43, no. 3, pp. 1110–1118, 2019.
- [50] X. Shu, L. Zhang, G.-J. Qi, W. Liu, and J. Tang, "Spatiotemporal co-attention recurrent neural networks for human-skeleton motion prediction," *IEEE Transactions on Pattern Analysis and Machine Intelligence*, vol. 44, no. 6, pp. 3300–3315, 2021.
- [51] R. Yan, L. Xie, X. Shu, L. Zhang, and J. Tang, "Progressive instance-aware feature learning for compositional action recognition," *IEEE Transactions on Pattern Analysis and Machine Intelligence*, 2023.
- [52] X. Shu, B. Xu, L. Zhang, and J. Tang, "Multi-granularity anchor-contrastive representation learning for semi-supervised skeleton-based action recognition," *IEEE Transactions on Pattern Analysis and Machine Intelligence*, 2022.
- [53] J. Tang, X. Shu, R. Yan, and L. Zhang, "Coherence constrained graph lstm for group activity recognition," *IEEE transactions on pattern analysis and machine intelligence*, vol. 44, no. 2, pp. 636–647, 2019.
- [54] P. Huang, X. Shu, R. Yan, Z. Tu, and J. Tang, "Appearance-agnostic representation learning for compositional action recognition," *IEEE Transactions on Circuits and Systems for Video Technology*, 2024.
- [55] J. Luo, Y. Li, Y. Pan, T. Yao, H. Chao, and T. Mei, "Coco-bert: Improving video-language pre-training with contrastive cross-modal matching and denoising," in *ACM MM*, 2021, pp. 5600–5608.
- [56] A. Radford, J. W. Kim, C. Hallacy, A. Ramesh, G. Goh, S. Agarwal, G. Sastry, A. Askell, P. Mishkin, J. Clark *et al.*, "Learning transferable visual models from natural language supervision," in *ICML*, 2021, pp. 8748–8763.
- [57] K. Zhou, J. Yang, C. C. Loy, and Z. Liu, "Conditional prompt learning for vision-language models," in *CVPR*, 2022, pp. 16 816–16 825.
- [58] H. Xu, G. Ghosh, P.-Y. Huang, D. Okhonko, A. Aghajanyan, F. Metze, L. Zettlemoyer, and C. Feichtenhofer, "Videoclip: Contrastive pre-training for zero-shot video-text understanding," in *EMNLP*, 2021.
- [59] C. Ju, T. Han, K. Zheng, Y. Zhang, and W. Xie, "Prompting visual-language models for efficient video understanding," in *ECCV*, 2022, pp. 105–124.
- [60] X. Wang, S. Zhang, J. Cen, C. Gao, Y. Zhang, D. Zhao, and N. Sang, "Clip-guided prototype modulating for few-shot action recognition," *International Journal of Computer Vision*, 2023.
- [61] O. Vinyals, C. Blundell, T. Lillicrap, D. Wierstra *et al.*, "Matching networks for one shot learning," in *NIPS*, vol. 29, 2016.
- [62] T. Brown, B. Mann, N. Ryder, M. Subbiah, J. D. Kaplan, P. Dhariwal, A. Neelakantan, P. Shyam, G. Sastry, A. Askell *et al.*, "Language models are few-shot learners," in *NIPS*, vol. 33, 2020, pp. 1877–1901.
- [63] S. Zheng, S. Chen, and Q. Jin, "Few-shot action recognition with hierarchical matching and contrastive learning," in *ECCV*, 2022, pp. 297–313.
- [64] X. Wang, S. Zhang, Z. Qing, C. Gao, Y. Zhang, D. Zhao, and N. Sang, "Molo: Motion-augmented long-short contrastive learning for few-shot action recognition," in *CVPR*, 2023, pp. 18 011–18 021.
- [65] K. He, X. Zhang, S. Ren, and J. Sun, "Deep residual learning for image recognition," in *CVPR*, 2016, pp. 770–778.
- [66] J. Deng, W. Dong, R. Socher, L.-J. Li, K. Li, and L. Fei-Fei, "Imagenet: A large-scale hierarchical image database," in *CVPR*, 2009, pp. 248–255.

- [67] L. Wang, Y. Xiong, Z. Wang, Y. Qiao, D. Lin, X. Tang, and L. Van Gool, "Temporal segment networks: Towards good practices for deep action recognition," in *ECCV*, 2016, pp. 20–36.
- [68] A. Vaswani, N. Shazeer, N. Parmar, J. Uszkoreit, L. Jones, A. N. Gomez, Ł. Kaiser, and I. Polosukhin, "Attention is all you need," in *NIPS*, vol. 30, 2017.